Title: To Bind or Not to Bind: diagnosing false positives for 1:1 binding to G-Protein

Aerin E. Baker,[1] Madison N. Hoogstra,[1] Noah J. Pehrson,[1] Anna E. Jipping,[1] Orin R. Daspit,[1] Magdalene A. Grabill,[1] Adelaide A. Stonehouse,[1] Douglas A. Vander Griend,[1] Federica Santoro,[2] Diego Brancaccio,[2] Laura Carosella,[3] Stefano Raniolo,[3] Vittorio Limongelli[3]

[1]*Department of Chemistry & Biochemistry, Calvin University, Grand Rapids, MI*

[2]*Department of Pharmacy, University of Naples, Italy*

[3]*Università della Svizzera italiana, Lugano, Switzerland*

Key Words: binding, false positive, thermodynamic modeling, global analysis, G-protein

Abstract

Binding studies are ubiquitous in chemistry, but their extensive usefulness is undermined by false positive and false negative results. Centering on the G-protein mini-Gs, we present a thorough study with both simulated and experimental spectrophotometric titration data to diagnose the validity of both binding and non-binding models. Without the use of statistical tests like Bayesian Information Criterion (BIC) and data reconstruction fractions, spurious binding models may go undetected. Furthermore, if the signal change upon binding is too minute, false negatives can also result. Delineating such issues is paramount to effective science.

Introduction

G-proteins represent one of the most important families of second messengers, serving as molecular switches in regulating vision, metabolism, neurotransmission mechanisms and many other processes vital to the normal physiology.[1] Inhibition of G-proteins has also been investigated for treatment of cancer, asthma, metabolic disorders, and other diseases.[2, 3, 4, 5] Whether it's signaling or inhibition, these pathways all require molecules to bind. The primary reaction of G-protein (Gp) is the hydrolysis of GTP to GDP. Only a few compounds are known to selectively disrupt the normal mechanism of activation of Gα, which is the subunit of Gp that binds GTP (Figure 1). The most notable are cholera[6] and pertussis toxins,[7] which are, respectively, an irreversible $G\alpha_i$ inhibitor and an irreversible $G\alpha_s$ activator. Additionally, drug molecules like YM-254890[8] and FR900359[9] are $G\alpha_q$ inhibitors that reversibly bind.

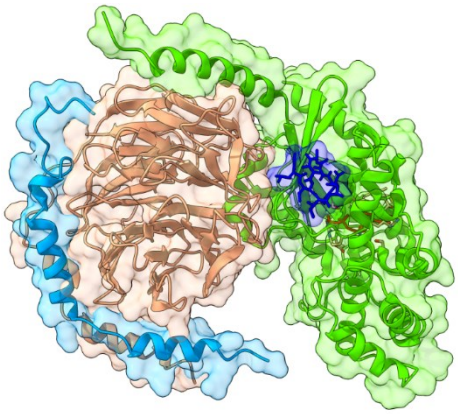

Figure 1. Inactive Gαβγ-GDP heterotrimer with YM-254890 inhibitor bound. The Gp subunits are represented as green (Gα), light orange (Gβ) and sky blue (Gγ) cartoons and surfaces. GDP is depicted as red sticks, whereas YM-254890 is shown as blue sticks and surface.

Measuring binding constants in biomolecular systems paves the way for further understanding and controlling biochemical pathways.[10, 11] Indeed, all chemical systems can benefit from this type of thermodynamic characterization.[12, 13]

The quantification of binding constants can be accomplished in various ways.[14] Usually, a solution of one type of molecule is titrated into another, while signal change is monitored. Isothermal Titration Calorimetry measures the total heat released by a system upon additions of a titrant.[15, 16, 17] Nuclear Magnetic Resonance monitors the shifting magnetic environments of the atoms and molecules involved.[18] Other spectroscopic methods—including UV-Vis,[19, 20, 21] fluorescence,[22, 23, 24] circular dichroism,[25] Raman,[26, 27] and infrared[28]—track the changing electronic structure of molecules upon binding. Each of these methods has its own limitations and advantages.

Regardless of the chosen method, quantifying binding constants can be troublesome.[29, 30, 31, 32, 32, 33, 34] It is possible to conduct a titration in which a signal change implies binding when, in fact, no binding occurred. This would be a false positive for binding. It is also possible to conduct a titration in which the signal change incorrectly implies no binding. This would be a false negative for binding. Both situations lead to unwanted consequences.

Many people have attempted to measure 1:1 binding.[35, 36, 37] In ACS journals alone, there are nearly 4,000 articles that include the phrase "1:1 binding." Just over 2% of these articles also mention the phrase "false positive" or "false negative."

In this work we present simulated and real spectrophotometric titration data. The data is globally modeled and statistically analyzed to dissect the various possible outcomes—both false positives and false negatives—when attempts are made to experimentally measure binding constants. Ultimately, key tools and chemical insights are presented for identifying and revamping titration experiments that lead to false conclusions about binding.

Methods

Reagents

Mini-Gs393, an engineered GTPase domain of the Gα subunit, (GIEKQLQKDKQVYRATHRLLLLGA DNSGKSTIVKQMRIYHGGSGGSGGTSGIFETKFQVDKVNFHMFDVGGQRDERRKWIQCFNDVTAIIFVVDSSDYNRLQEALNDFKSI WNNRWLRTISVILFLNKQDLLAEKVLAGKSKIEDYFPEFARYTTPEDATPEPGEDPRVTRAKYFIRDEFLRISTASGDGRHYCYPHFTCAV DTENARRIFNDCRDIIQRMHLRQYELL) was expressed and purified by Dr. Federica Santoro from the Prof. Vittorio Limongelli's group at the Faculty of Biomedical Sciences, Università della Svizzera italiana (USI) in Lugano, Switzerland. Upon lyophilization, NMR confirmed that it remained folded in solution. After shipping in dry ice to the United States, each sample was reconstituted in 2 mL of nanopure water to obtain a mini-Gs concentration of 37 μM with a pH 7.5 buffer concentration of 10 mM HEPES buffer, 100 mM NaCl, 1 mM $MgCl_2$, 1 μM GDP, and 0.1 mM TCEP.

GDP (Guanosine-5'-diphosphate disodium salt, *AmBeed*, 98.80 % purity), ADP (Adenosine-5'-diphosphate disodium salt dihydrate, *Chem-Impex Int'l Inc*., 98.3 % purity), caffeine ($C_8H_{10}N_4O_2$, Sigma-Aldrich, ≥ 99.0% purity), BIM-46187 hydrochloride ((2R, 2'R)-3, 3'-dithiobis[2-amino-1-[(8S)-8-(cyclohexylmethyl)-5, 6-dihydro-2-phenylimidazo[1, 2-a]pyrazin7(8H)-yl]-1-propanone,

tetrahydrochloride, *Cayman Chemical*), $Ni(ClO_4)_2 \cdot 6H_2O$ (*Strem Chemicals, INC*., 99 wt%), and $Cu(ClO_4)_2 \cdot 6H_2O$ *(Sigma-Aldrich*, 98 wt%) were used without further purification. CDS023730 (3-[3-(Aminomethyl)phenyl]-5-Me-6, 7-dihydroisoxazolo[4, 5-*c*]pyridin-4(5*H*)-hydrochloride) was provided by Prof. Vittorio Limongelli.

Preparation of solutions

All Gs titrations were conducted with aqueous ~3.7 μM Gs analyte solution made from a ~1 mL of the above reconstituted Gs solution and ~9 mL of buffer (10 mM NaHEPES, 100 mM NaCl, 1 mM $MgCl_2$, and 0.1 mM TCEP). All Gs analyte solutions started with one equivalent of GDP bound as synthesized.

GDP solutions had concentrations of ~80 μM and were made up with the same 7.5 pH buffer. This GDP solution was the titrant for the GDP titrations as well as the basis buffer for other titrant solutions (BIM, CDS, caffeine).

The ADP solution had a concentration of ~ 70 μM and was made up with the GDP-containing buffer.

BIM solutions in the GDP-containing buffer had concentrations of ~110 μM. Dataset H had a BIM titrant that was made up with the non-GDP-containing buffer. < 5% acetonitrile was added to the BIM titrants to ensure full dissolution of BIM.

CDS solutions in the GDP-containing buffer had concentrations of ~ 105 μM.

Caffeine solutions in the GDP-containing buffer had concentrations of ~ 200 μM.

Aqueous solutions of Cu(II) and Ni(II) had a concentrations of ~8 mM.

More specific details for each titration experiment's solutions can be found in the Supporting Information.

Titrations

Twenty-five spectrophotometric titrations were performed by titrating with aqueous solutions of varying reagents. Absorbance data for Gs titrations were typically taken every nanometer from 240 nm to 330 nm. Details for each titration can be found in the Supporting Information.

Spectrophotometry

Two different spectrometers were used to collect data: an OLIS 14 UV/VIS/NIR and a Hitachi U-3900H. All data were collected around 296 K relative to a baseline of buffer solution or deionized water to match the sample. Absorbance scans were taken after each addition of titrant.

Chemometric Modeling

All titration datasets were analyzed using *Sivvu* to model spectrophotometric titration data, either allowing for binding or not. This approach treats the data as a two-dimensional matrix of numbers (ABS) with each chemical solution being a distinct column of data. One dimension is the wavelength, w. The other dimension is the number of distinct chemical solutions, s. This matrix can be factored into two smaller matrices (ε and C) that model the data while leaving some residual unaccounted for.[38]

$$\text{ABS}\ (w \times s) = \varepsilon\ (w \times f) \cdot C\ (f \times s) + \text{Residual}\ (w \times s) \quad (1)$$

$$w \equiv \text{number of wavelengths}$$

$$s \equiv \text{number of chemical solutions}$$

$$f \equiv \text{number of factors}$$

The number of data points in the dataset is ws. The number of factors is either two or three—corresponding to non-binding or binding, respectively—for all the datasets in this work. Together, the ε and C matrices constitute the model of the data. They can represent the molar absorptivity values and the molar concentration values if sufficient restrictions are applied during the fitting process. The total number of values in the model is wf + fs, which is an order of magnitude less than the number of data points. Depending on the type of model used, some of these values are independent parameters while others are determined from various mathematical relationships that are imposed on the model. The number of model parameters depends on the number of independent values used to determine the ε and C matrices.

To model the data without any chemical restrictions, all the elements of ε and C are free parameters. This means there are wf + sf parameters in the model. Singular value decomposition (SVD) is used to find the resulting ε matrix. Then least squares optimization is used to find the C matrix that leads to the minimal residual. There are no restrictions on the values in either the ε or the C matrix when modeling the data this way, which is why these models are referred to as unrestricted.

To chemically model binding, SIVVU uses Parametric Equilibrium Restricted Global Analysis (PERGA)[39, 40, 41] to constrain C (the concentration matrix), using mass balance and equilibrium. The number of factors, f, is now the number of distinct chemical species. For the non-binding model, f = 2, and the entire C matrix is determined by the amount of host and guest in the system, so the number of parameters in the model is just 2w. For the binding model, the number of parameters is technically 3w + 1 since now there is a third chemical species, the complex. The 3w parameters are the molar absorptivity values for the host, guest, and complex, and they are determined through non-negative least squares fitting. The one additional parameter is the associative binding constant, which is used to parameterize the concentration matrix where the equilibrium amounts of host, guest, and complex always need to satisfy the standard relationship $[\text{Complex}]_{eq} = K_a[\text{Host}]_{eq}[\text{Guest}]_{eq}$.[42] *Sivvu* also calculates the 95% confidence intervals on the logK values using bootstrapping—done 100 times for all proposed models.[43] These two models are referred to as restricted because the binding constant parameter greatly restricts the model.

For each dataset, the unrestricted binding model, U_3, the restricted binding model, R_3, the unrestricted non-binding model, U_2, the restricted non-binding model, R_2, are compared to ascertain whether the data supports the existence of a third factor and whether or not it is the 1:1 complex. Obviously, the more parameters in the model, the more data that can be accounted for. U_3 has the most parameters and is followed by R_3, since w is generally much greater than s. Next is U_2 followed by R_2. The crucial question is whether a third chemical species, specifically the 1:1 complex of host and guest, exists. Ultimately, we aim to identify the cases in which the chemically

binding model, R_3, is merited above the others, meaning that there is a third factor in the data and that it is best modeled as a 1:1 complex of host and guest.

Simulated Data

Artificial datasets were constructed in Microsoft Excel so that the binding constant could be known and controlled. The molar absorptivity curves for host (H), guest (G), and complex (HG) were each set as a distinct Gaussian function. The same host curve and same guest curve were used throughout the simulations. The curve for the complex was adjusted to alter the degree to which it varied from the sum of the host and guest curves. The total absorbance was designed to be less than 1.0 ABS. Noise was added to the dataset by multiplying the absorbance values by random values from a normal distribution with a mean of 1 and a standard deviation of 0.01. This produces errors that scale with the absorbance values themselves.

Sixteen datasets were differentiated based on two parameters: the distinctiveness of the complex's absorptivity curve and the strength of the binding regime. The former is defined as the vector angle between the molar absorptivity curve of the complex and the sum of the curves for the host and the guest, with values of 0°, 3°, 9°, and 27°. The latter is quantified as $\log([H_{total}]K_a)$,[29, 30] with values of 1, -1, -3, -5. As a result, the final percent bound ranged from 96.8% down to 0.004% when four equivalents of guest present. Three additional datasets were constructed (3a, 6a, and 7a) based on three of the original 16 to explore the impact of error on binding detection. 3a has lower total error factored in (0.001). 6a was expanded to range over more equivalents of guest, which increased the total ABS beyond 3 and consequently introduced more error. 7a has a higher total error factored in (0.2).

Statistical Analysis

The restricted and unrestricted models with either two or three factors are distinguished by the number of model parameters, which is the number of values that can be adjusted in attempts to fit the data. To compare the four different models for each dataset, numerous criteria were invoked.[44]

SVD: The number of additive orthogonal mathematical factors that exist within the data can be determined using singular value decomposition (SVD).[45] This is a purely mathematical way to factor any rectangular matrix into orthogonal components by expressing it as the product of three matrices, one of which represents the weight of each additive factor in the data. These are the S-values. If a factor weight is more than twice that of the next largest factor, it is counted as a significant factor along with every factor larger than it. If a factor weight is less than twice but greater than 30% of the next largest factor, it is possibly significant. All remaining factors are deemed insignificant, corresponding to random noise. Each significant factor points to a feature in the data that might represent a chemical species or some other artifact in the data such as baseline shifts, instrument drift, non-equilibration, or human error.

LogK±(confidence intervals): For chemically binding (R_3) models, Sivvu optimizes the associative binding constant, K, that best fits the data (reported as logK). 100 bootstrap calculations are run to generate a 95% confidence interval for the logK.[42] The larger the logK value, the stronger the

modeled binding between host and guest. The tighter the confidence intervals, the more consistently the binding constant is supported by the random shufflings of the data.

Angle: For every R_3 binding model, a molar absorptivity curve (ε) for H, G, and HG is generated. Angle refers to the vector angle between the curve for HG and the sum of the curves for H and G. A smaller angle indicates more similarity between these two curves, meaning that the HG approaches the sum of the H and G curves.

$$\cos(\theta) = \frac{2\cdot(\overrightarrow{\varepsilon_H}+\overrightarrow{\varepsilon_G})\cdot\overrightarrow{\varepsilon_{HG}}}{(\overrightarrow{\varepsilon_H}+\overrightarrow{\varepsilon_G})^2+(\overrightarrow{\varepsilon_{HG}})^2} \tag{2}$$

a±: The non-linearity of each dataset can be quantified by calculating the magnitude and error of the quadratic coefficient when fitting the change in average absorbance over the span of the titration. If the error range on *a* includes zero, this supports non-binding, indicating that the data cannot be fit any better quadratically than linearly. Consequently, the two-factor non-binding model would be preferred because it does not overfit the data. The magnitude of this term corresponds to the definitiveness of its conclusion.

$$\frac{1}{w}\sum_{w_{initial}}^{w_{final}} ABS_{ws} = a\left(\frac{[G]_{total,s}}{[H]_{total,s}}\right)^2 + b\left(\frac{[G]_{total,s}}{[H]_{total,s}}\right) + c \tag{3}$$

$$ABS_{ws} \equiv absorbance\ data\ at\ wavelength\ w\ and\ solution\ number\ s$$

ΔΔ: The unrestricted root-mean-square-residual (uRMSR) is the error of the unrestricted fit, which is necessarily lower than the restricted RMSR (rRMSR). A merited chemical species will lower the rRMSR value as least as much as a third factor lowers the uRMSR value. The ΔΔ value represents how much the binding model ($RMSR_3$) closes the residual error gap relative to the non-binding model gap.

$$\Delta\Delta = (rRMSR_2 - uRMSR_2) - (rRMSR_3 - uRMSR_3) \tag{4}$$

A positive ΔΔ value establishes the chemical legitimacy of the bound species. A negative ΔΔ value indicates that the complex is not chemically legitimate and, therefore, the binding model is not supported by the data. The magnitude of this term corresponds to the definitiveness of its conclusion.

ΔΔrecon: The fraction of data that can be reconstructed can be calculated for any model. This is done by taking the sum of the S-values from the SVD *for the model* relative to the number of chemical solutions, s.

$$recon_f = \frac{1}{s}\sum_{i=1}^{f} Svalue_i \tag{5}$$

This value approaches unity as the model improves. A higher reconstruction fraction indicates that the model fits the data more closely. Reconstruction fraction always increases with additional added species, so it is the gaps between the restricted reconstruction of the model and the unrestricted reconstruction of the data that are calculated (Δrecon). Then, if this gap decreases

(ΔΔrecon > 0) with the binding model, the 1:1 chemical species is merited. The magnitude of this term corresponds to the definitiveness of its conclusion.

$$\Delta\Delta recon = (urecon_2 - rrecon_2) - (urecon_3 - rrecon_3) \quad (6)$$

Solutions (#) in the 20-80% range: A binding titration moves the amount of complex from a lower percentage, typically zero when starting with pure host, to a higher percentage as guest is titrated in. Since the chemical solutions that fall between 20% and 80% are the most useful for quantifying the binding constant, [29] they are the most sensitive to the value of the binding constant.[30] If a fit results in too few (< 8) chemical solutions in the 20-80% range, this indicates that the titration is not well-suited to quantify the binding constant.

F_{23} (and $F_{critical}$): An F-test, which compares variances, can be used to compare two nested models of a given dataset.[46, 47] In this case, the F_{23} is the F-statistic generated from the chemical binding (R_3) and non-binding (R_2) models. This value is compared to $F_{critical}$ value for $\alpha = 0.05$. If $F_{23} > F_{critical}$, then the F-statistic for the binding model is statistically significant, and the binding model is merited and preferred. If $F_{23} < F_{critical}$, then the binding model is not supported. The magnitude of this term corresponds to the definitiveness of its conclusion.

$$F_{ij} = \frac{(RMSR_i)^2 - (RMSR_j)^2}{(RMSR_j)^2} \cdot \frac{ws - p_j}{p_j - p_i} \quad (7)$$

$$\mathrm{p} \equiv \text{number of model parameters}$$

ΔAIC_{23}: The Akaike Information Criterion (AIC) quantifies the amount of information loss for a particular model relative to the data.[48] It is a formulation designed to compare models with many parameters, some of which may be extraneous.[49] It can be calculated based on the residual error between the data and the model, RMSR, with each parameter carrying a penalty of two.[50]

$$AIC_f = 2wsln(RMSR_f) + 2(p_f) \quad (8)$$

Its application to mathematical problems of this nature with two-dimensional structure is not decidedly defined.[51] We believe it is appropriate for comparing the 2-factor (U_2) and 3-factor (U_3) unrestricted models because they are more open-ended and consist of many parameters that do not necessarily have scientific meaning.

$$\Delta AIC_{23} = 2wsln(rRMSR_2/rRMSR_3) - 2(w + s) \quad (9)$$

The larger the value of ΔAIC_{23} value, the more a third factor is merited.

ΔBIC_{23}: The Bayesian Information Criterion (BIC) quantifies the unexplained variation in the dependent variable for a particular model.[53] While similar to AIC, it is formulated for qualitatively different situations: it is designed to compare nested models that depend on a relatively small number of parameters as the penalty term is considerably greater, helping to either confirm or falsify a model.[52]

$$BIC_f = 2wsln(RMSR_f) + \ln(ws)p_f \quad (10)$$

Also, like AIC, its application to mathematical problems of this nature with two-dimensional structure is not decidedly defined.[55] We believe it is appropriate for comparing the binding (R_3) and non-binding (R_2) chemical models because they are essentially the same except for the addition of the binding constant parameter. Furthermore, since the result at every wavelength is essentially the same with respect to binding vs non-binding, we apply the criterion only to the range of chemical solutions, *i.e.* w = 1.

$$\Delta BIC_{23} = 2sln(rRMSR_2/rRMSR_3) - \ln(s) \quad (11)$$

A positive ΔBIC_{23} value indicates that the 1:1 complex is merited in the model. Note that if the wavelength dimension is included in the calculation, the results maintain their relative comparisons but all the values of ΔBIC_{23} shift to positive numbers making interpretation more ambiguous. The impact of the single binding constant parameter also lessens.

Results & Discussion

Simulated Data

Nineteen artificial datasets were successfully modeled with PERGA, each in four ways: chemically restricted and binding (R_3), chemically restricted and non-binding (R_2), unrestricted and binding (U_3), and unrestricted and non-binding (U_2). Subsequently, a plethora of statistical analyses were performed on the fits of the data with the four models (Table 1).

Table 1. The details of 19 simulated datasets along with various model parameters and statistical test values. Bolded values indicate that binding is supported by the respective statistical test.

	Dataset Details					Model Results								
Dataset	LogK	LogHK	Data angle (°)	% Bound	SVD (sig, semi-sig)	LogK	LogK 95% CI	Model angle (°)	a ± ($\times 10^5$)	$\Delta\Delta$ ($\times 10^4$)	$\Delta\Delta$recon ($\times 10^4$)	F_{23} ($F_{critical}$ = 4.04)	ΔAIC_{23} (U2-U3)	ΔBIC_{23} (R2-R3)
1	5	1	27	96.8	3, 0	4.99	(4.97, 5.00)	27	**330 ± 20**	**4.33**	**260**	**2185**	**74000**	**192**
2	5	1	9	96.8	3, 0	5.00	(4.96, 5.04)	9.0	**48 ± 3**	**9.66**	**0.8**	**130**	**16629**	**63**
3	5	1	3	96.8	3, 0	4.92	(4.64, 5.05)	3.1	**-60 ± 10**	-0.04	-0.6	**14**	**5749**	**9**
3a	5	1	3	96.8	3, 0	5.00	(4.99, 5.03)	3.0	**-6.2 ± 0.4**	**0.01**	0	**1423**	**86246**	**171**
4	5	1	0	96.8	2, 0	2.88	(2.91, 3.14)	27	0.32 ± 0.9	-0.6	-11	1.0	947	-3
5	3	-1	27	27.2	2, 0	3.08	(3.01, 3.14)	25	**16 ± 0.8**	**174**	**0.9**	**28**	946	**19**
6	3	-1	9	27.2	2, 0	2.93	(2.95, 3.15)	27	**2.5 ± 0.9**	-0.5	-11	1.2	925	-3
6a	3	-1	9	65.9	2, 0	2.67	(2.66, 2.86)	29	**0.8 ± 0.1**	-2.0	-13	1.9	**1327**	-2
7	3	-1	3	27.2	2, 0	2.90	(2.91, 3.16)	25	4 ± 90	-0.6	-11	1.0	953	-3
7a	3	-1	3	27.2	2, 0	3.84	(3.74, 3.94)	37	6.3 ± 17	-12	-130	0.8	958	-3
8	3	-1	0	27.2	2, 0	2.88	(2.91, 3.15)	27	0.32 ± 0.9	-0.6	-11	1.0	947	-3
9	1	-3	27	0.40	2, 0	2.88	(2.92, 3.12)	27	0.32 ± 0.9	-0.6	-11	1.0	948	-3

10	1	-3	9	0.40	2, 0	2.88	(2.91, 3.20)	27	0.32 ± 0.9	-0.6	-11	1.0	950	-3
11	1	-3	3	0.40	2, 0	2.88	(2.91, 3.13)	27	0.32 ± 0.9	-0.6	-11	1.0	947	-3
12	1	-3	0	0.40	2, 0	2.88	(2.90, 3.13)	27	0.32 ± 0.9	-0.6	-11	1.0	947	-3
13	-1	-5	27	0.004	2, 0	2.88	(2.90, 3.14)	27	0.32 ± 0.9	-0.6	-11	1.0	947	-3
14	-1	-5	9	0.004	2, 0	2.88	(2.91, 3.15)	27	0.32 ± 0.9	-0.6	-11	1.0	947	-3
15	-1	-5	3	0.004	2, 0	2.88	(2.90, 3.15)	27	0.32 ± 0.9	-0.6	-11	1.0	947	-3
16	-1	-5	0	0.004	2, 0	2.88	(2.92, 3.10)	27	0.32 ± 0.9	-0.6	-11	1.0	947	-3

Every simulated dataset seemingly modeled well via PERGA with a logK of at least 2.88, corresponding to a minimal RMSR that could be achieved with the chemical binding model, R_3. At the host concentration level of 0.0001 M, this indicates binding of at least ~25% of the 1:1 complex by the end of the titration. Furthermore, the confidence intervals for the binding constants are all quite tight and reasonable. Without prior knowledge of the binding constant, it would be expected that an experimentalist could easily be convinced that each of these titration experiments evidenced substantial binding of the guest to the host.

Concerningly, though, half of these simulated datasets were constructed with a logK value much smaller than the binding model would suggest. False positives such as these should cause great concern.

For datasets 9 – 16, the 1:1 complex does not actually form to any substantial extent; however, the apparently satisfactory R_3 model implies that it does. This is because the existence of the complex allows the model to account for random noise in the data. Obviously, any additional species allows the model to account for more of the data, whether signal or noise. Even with the chemical restriction that forces the third species to be the 1:1 complex, if the model uses a molar absorptivity curve that is simply a sum of the host and guest curves, it can utilize this extra curve to address extra error without negatively impacting the fit. Such a curve does not even manifest as a distinct factor in the SVD analysis as it is not additively distinct.

SVD can identify the third contributor if it is sufficiently distinct above the noise level. Otherwise, it can't be distinguished even if it is real. This is demonstrated by datasets 4 through 8.

Fortunately, there exist additional statistical tools that can help diagnose such insidious false positives.

First, it is possible to assess the degree of non-linearity in the spectrophotometric dataset to see how warranted a quadratic fit is. The more the quadratic coefficient *'a'* deviates from zero, the less the linear fit is sufficient. For the false positive cases noted above, the error range on 'a' includes zero because there is in fact no third species. The reason that '*a*' would be non-zero is because the absorbance change for a dataset is non-linear as it is comprised of at least three spectroscopically distinct signatures. This is evident in datasets 1, 2, 3, 3a, 5, 6, and 6a which legitimately show binding. Note that for dataset 6, the '*a*' coefficient is the only statistic that corroborates binding.

Second, ΔΔ captures the degree to which the chemical binding model closes the error gap on the unrestricted binding model. According to this statistic, models for datasets 1, 2, and 5 verify binding. Datasets 3 and 3a are borderline. The remaining datasets show no binding.

Similarly to ΔΔ, ΔΔrecon captures the extent to which adding a 1:1 complex to the model can decrease the gap between the restricted and unrestricted reconstructions of the data. According to this statistic, models for datasets 1, 2, and 5 verify binding. Again, datasets 3 and 3a are borderline, and the remaining datasets show no binding.

Next, F_{23} can be compared to $F_{critical}$ to decide between binding and non-binding.[53] According to this statistic, models for datasets 1, 2, 3, 3a, and 5 verify binding. The remaining datasets show no binding. Notice that for 3a, having a higher signal to noise ratio than dataset 3 vaults the F_{23} statistic by two orders of magnitude.

Finally, ΔAIC_{23} and ΔBIC_{23} quantify the amount of chemical information gained upon adding a third species. According to both statistics, models for datasets 1, 2, 3, and 3a verify a third factor, which is the 1:1 complex. ΔAIC_{23} further indicates that dataset 6a merits a third factor. ΔBIC_{23} indicates that dataset 5 merits the 1:1 complex as the third factor. The remaining datasets do not merit a third factor of any kind.

There are two borderline datasets that warrant additional consideration. Dataset 3 fails two of the five statistical tests for binding despite being built with 97% binding. This occurs because the molar absorptivity curve for the complex is too similar to that of the sum of the host and guest curves to be successfully resolved. Decreasing the intrinsic error level in the raw absorbance data by a factor of 10 rectifies this issue, as exemplified by dataset 3a, which shows binding according to all five statistical tests. Dataset 6 fails four of the five tests despite 27% binding and a relatively distinct curve for the bound species. Normally, increasing the number of equivalents would be advantageous because it increases the binding fraction.[29, 30] However, with an absorbing guest, the resulting absorbance increases, thus increasing the amount of error in the data as expected for spectrophotometric experiments. Dataset 6a, which extends the titration to 20 equivalents—and consequently exhibits a maximum absorbance of 4—actually fails the same four tests even more decisively. The existence of a guest that absorbs is central to this predicament; otherwise, distinguishing between binding and non-binding is trivial.

Finally, dataset 7a represents a special case in which the modeled binding constant is again too large but leads to a model in which the amount of complex formed is 70% at the end of the titration. This is sufficiently saturated to convince an experimentalist that the experiment is appropriately designed to assess the corresponding level of binding.

So, troublesomely, false positive binding experiments clearly exist. There are experiments without binding that model notable binding, and there are experiments that have modest binding that model considerable binding. For the former, an astute chemist would repeat titration experiments going out to further equivalents. For the latter, the result is convincing as it stands because the complex appears to form to a sufficient level of saturation, and the only hope of detecting a false positive in this case is to run statistical tests. The aforementioned six statistics can help delineate them as all point to non-binding even with a tempting binding model (R_3). Clearly, all these statistics should be checked before binding is declared. With data that is decidedly two or three factors, the a-parameter test appears to work best. Unfortunately, real data will often have additional non-chemical factors that render some of the statistical tests less helpful.

False negatives also exist: when binding happens but the model of the data does not show it. This is due, almost exclusively, to the fact that the molar absorptivity curve of the complex is just a linear combination of the respective host and guest curves. This is exhibited best with dataset 4 for which the binding should be substantially larger but the modeling does not detect it because the complex curve is too similar to those of the host and the guest. The existence of complex curves that are just the sum of the curves of their component molecules would suggest that the electronic structure of the complex is unperturbed relative to the that of its components. This begs the question as to whether chemical binding has actually taken place.

Experimental Data

To put these various statistical analysis techniques to the test, the same above analyses were conducted on 25 *in vitro* titrations with various titrants and analytes. The majority of these titrations study how Gs binds (or doesn't) to various drug and biochemical molecules (Table 2). GDP is expected to bind.[54] BIM and CDS both were predicted to bind.[55] All other titrations were expected to not show binding.

Table 2. Twenty-five *in vitro* spectroscopic titrations and their respective statistical outputs when fit with binding/non-binding models. Datasets A-D are Gs titrated with GDP. Datasets E-H are Gs titrated with BIM. Datasets I-M are Gs titrated with CDS. Datasets N-S are Gs titrated with caffeine. Datasets T-U are Gs titrated with ADP. Dataset V is caffeine titrated with BIM. Dataset W is BIM titrated with caffeine. Dataset X is Ni(II) titrated with Cu(II), and Dataset Y is Cu(II) titrated with Ni(II). The number of chemical solutions that are modeled with a percentage of possible complex between 20% and 80% is shown in the final column, except for Datasets A-D because those were necessarily started at one equivalent of guest. Bolded values indicate binding according to the statistical test.

Dataset	SVD (sig, semi-sig)	Temperature	LogK	LogK 95% CI	Angle (°)	a± (× 10^4)	ΔΔ (×10^4)	ΔΔrecon (×10^4)	F_{23}	$F_{critical}$	ΔAIC_{23} (U2-U3)	ΔBIC_{23} (R2-R3)	# Solutions in 20-80% range
A	3, 0	296	5.09	(4.89, 5.56)	28.6	**-7.1 ± 0.6**	**16**	**1.3**	**625**	4.08	11487	**117**	N/A
B	4, 1	296	5.57	(5.01, 5.75)	15.4	**-5.2 ± 0.3**	**5.2**	**0.2**	**148**	4.21	5102	**52.6**	N/A
C	4, 1	296	5.36	(5.18, 5.58)	48.5	**-17 ± 1.2**	**3.6**	**0.2**	**460**	4.21	6344	**83.4**	N/A
D	4, 4	299	6.51	(6.40, 13.99)	71.3	**-2.9 ± 0.4**	**34**	**209**	**546**	4.08	10195	**113**	N/A
E	4, 0	296	4.40	(3.70, 4.94)	35.2	**-28 ± 1**	**5.7**	-20	**59.0**	4.26	6575	30.2	17
F	4, 2	296	6.05	(4.00, 14.21)	3.3	**-2.4 ± 0.1**	**2.7**	-0.4	**33.4**	4.20	2927	20.9	2
G	4, 1	296	4.84	(3.84, 5.85)	2.2	**-4.4 ± 0.3**	-3.7	-2.5	**7.2**	4.17	2047	3.6	29
H	5, 2	299	5.13	(4.15, 5.52)	36.0	**-6.9 ± 0.3**	**15**	-6.2	**111**	4.24	2605	44.1	25
I	2, 0	298	4.79	(-6.22, 12.21)	1.2	**-37 ± 2**	**6.1**	-2.2	**12.6**	4.45	380	8.1	16
J	3, 2	296	4.83	(-6.28, 6.22)	11.8	**-71 ± 0.4**	**3.1**	-0.7	**41.6**	4.38	4027	22.4	17
K	5, 0	296	6.34	6.03, 7.59)	2.6	-0.2 ± 0.6	**32**	**3.0**	**245**	4.18	4551	**68.4**	3
L	3, 3	299	5.61	(5.44, 5.84)	3.7	**-4.7 ± 0.3**	-9.1	-1.2	**98.4**	4.24	9554	41.4	5
M	3, 4	299	5.74	(5.55, 6.08)	5.9	**-6.9 ± 0.6**	-27	-33	**94.7**	4.21	14825	41.8	6
N	2, 4	296	4.62	(3.85, 11.78)	2.2	**-2.1 ± 0.2**	-1	-1.4	4.1	4.30	1287	1.0	19
O	3, 0	296	4.68	(4.22, 5.45)	1.1	**-1.3 ± 0.2**	**3.5**	-1.0	**31.5**	4.30	1736	19.0	20
P	4, 2	296	6.54	(3.56, 14.06)	0.8	**-2.7 ± 0.9**	**2.4**	-1.5	**8.8**	4.20	1626	5.0	3
Q	3, 3	296	5.58	(5.16, 6.18)	0.5	**-4.4 ± 0.1**	**0.2**	-0.6	**35.2**	4.26	3496	21.1	6
R	3, 3	296	7.72	(5.99, 11.97)	4.1	**-1.6 ± 0.8**	**19**	**8.4**	**120**	4.18	4628	49.0	2
S	2, 4	296	4.15	(-3.73, 6.00)	8.4	**-4.0 ± 0.4**	-0.8	-2.8	**5.0**	4.21	1463	1.7	7
T	4, 2	299	5.09	(5.00, 5.22)	66.6	**-86 ± 15**	**26**	-3.0	2	4.17	4544	**66.4**	29
U	2, 4	299	6.96	(5.80, 13.57)	9.3	**-12 ± 0.5**	**20**	**8.9**	**115**	4.18	1147	47.8	2
V	4, 0	299	7.74	(4.53, 17.42)	1.1	**-14 ± 0.3**	-1.3	-5.3	**5.3**	4.13	3329	1.7	1
W	4, 2	299	5.24	(5.12, 5.42)	73.8	**-2.9 ± 0.4**	**3**	-47	**34.3**	4.12	9467	22.3	35
X	2, 3	298	0.40	(0.26, 2.49)	45.3	**-10 ± 0.3**	-0.8	-7.3	2.3	4.21	6740	-0.9	0
Y	3, 1	295	1.45	(1.15, 1.67)	1.9	**-1.5 ± 0.1**	-1.1	-27	3.3	4.23	14371	0.1	23

For all these experiments except datasets X and Y, the optimized logK value suggests significant binding occurred for the respective host concentration. SVD analysis, in all cases except for Dataset I, exhibits at least one additional factor beyond the first two—host and guest. Targeted statistical analyses, however, indicate that many of these experiments are likely false positives for binding.

SVD is not a good tool for diagnosing false positives or negatives because many data artifacts, chemical or otherwise, can appear. Note in Table 2 that some experiments yield up to eight semi/significant factors. A binding model can take advantage of this, using the new parameter (the 1:1 complex) to account for some of that extra error present in the data, falsely presenting a "better" model that appears to show binding where there is none. Also, if the discrepancy between the molar absorptivity curve for the complex and the sum of the curves for its host and guest components is too small, a false negative result emerges because no binding can be detected even when it should be.

The quadratic coefficient 'a' is also undiscriminating with false positives because most real datasets include additional factors (baseline shifts, instrument drift, non-equilibration, human error) that defy the pure linearity of a non-binding model.

For these above datasets, ΔΔ is quite inconsistent even for replicate experiments with a common titrant, with the exceptions of GDP and ADP. This statistical criterion seems to be easily obfuscated by the presence of non-random error.

ΔΔrecon, however, behaves much more consistently and seems to indicate nonbinding for all titrants except GDP. Because this term focuses on the positive reconstructive ability of the model, it appears to be less sensitive to residual error in the data.

Like 'a', F_{23} is undiscriminating with these real datasets. 19 out of 21 of the Gs titrations yield an F_{23} value that is higher than $F_{critical}$. Bardsley *et al*. claim that while an F-test is not strictly appropriate with non-linear models, it is still useful if the number of parameters is less than three.[45] In this case the number of non-linear parameters is just 1 or zero as the other parameters behave linearly. The same statistical analysis can be done on just one dimension of the model—namely the chemical solutions—with highly comparable numerical results. Regardless, this analysis often doesn't match either the other statistical analyses or chemical expectations.

ΔAIC_{23} and ΔBIC_{23} appear to behave somewhat reliably with real data, however the tipping point between binding and non-binding is ambiguous, especially for the former. Datasets with an ΔAIC_{23}, value around 10,000 seem to support binding. Smaller values around 1000 point to non-binding. Datasets with an ΔBIC_{23} value above 50 seem to support binding. All four GDP titrations support binding. Three out of the five CDS titrations seem to support binding according to this statistic. ADP titration datasets may also support binding. All other titrations seem to not support binding.

Conclusion

Among all the titrants in Table 2, GDP is the only one for which we can definitively conclude that it binds to Gs. All statistical indicators, especially ΔΔrecon and ΔBIC_{23} affirm binding. The logK values for the binding average out to 5.6 with 95% confidence interval from 4.9 to 12.1. (The 90% confidence interval is 5.0 to 7.5). Using Gα purified from bovine brain, Higashijima *et al*. found the logK to be 7.5.[56]

BIM, however, does not appear to bind to Gs, because both ΔΔrecon and ΔBIC_{23} show non-binding for all four replicates. Furthermore, Dataset F has only two chemical solutions in the 20% - 80% sensitivity zone (Figure 2), which means that this experiment is inconclusive and should be rerun at a lower concentration of host, which will lead to many more chemical solutions with 1:1 complex between 20% and 80% if the binding is real.

The initial conclusion for CDS is somewhat ambiguous. For one of the five replicates (K), both ΔΔrecon or ΔBIC_{23} show binding. Replicates L and M have moderately high ΔBIC_{23} values too. However, these three experiments lack a sufficient number of chemical solutions in the 20% - 80% sensitivity zone for binding quantification. Therefore, more data should be taken with chemical solutions that contain between 20% and 80% of the possible 1:1 complex. If binding is indeed

happening, these titration experiments will better confirm it. Otherwise, they should evidence non-binding. Because the models for datasets K, L, and M only exhibit a small number of chemical solutions within the 20% - 80% range, we focus on Datasets I and J, which contain more high-sensitivity chemical solutions, to judge that CDS likely does not bind to Gs.

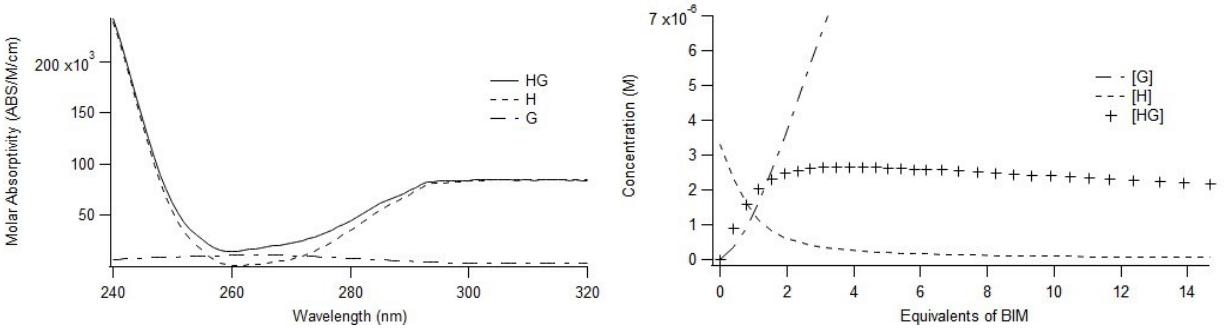

Figure 2. Molar absorptivity curves (left) and concentration profiles (right) for dataset F. Note how the curve for HG appears to be the sum of the curves for H and G. Also note how only the second and third solutions are within the 20-80% bound range.

We judge that caffeine does not bind to Gs as both ΔΔrecon and ΔBIC_{23} show non-binding except for with Dataset R, which has only 2 chemical solutions in the 20% - 80% bound range. Additional titration experiments that focus on this region will likely corroborate non-binding. Also, the logK value for the model of Dataset R is anomalously high, further indicating that the binding is spurious.

ADP exhibits one experiment (Dataset T) that supports binding. Dataset U has only has two solutions in the 20% - 80% bound range. Additional experiments are needed to establish a definitive conclusion for this substrate.

The final four experiments involve reagents that should not bind to each other at all. While some logK values as well as 'a' and several other statistical tests point to binding, ΔΔrecon and ΔBIC_{23} show non-binding as expected.

As can be seen from the models of real titration experiments, false positives exist and can be tricky to identify. By creating a dummy complex with a molar absorptivity curve that mimics those of the host and guest, a model accounts for more error. If, according to the model, the number of chemical solutions that present 1:1 complex in the 20% - 80% bound range is small, then additional titration data should be acquired. This range has been identified as especially important for quantifying binding constants because it is the chemical solutions in this range that are most sensitive to the binding constant value.[30] Any titration that is used to support binding should include at least 8 – 10 chemical solutions in this range. Even when this number is satisfactorily high though, the 1:1 binding model may still be unmerited. It is crucial to check the statistical criteria to confirm the veracity of the binding model. In particular, ΔΔrecon seems to be the most consistently dependable, with positive values when the binding model outperforms a non-binding model, and negative values when it doesn't. ΔBIC_{23} also can helpfully identify when a binding chemical model overfits the data.

False negatives are also hypothetically possible, but not expected in real datasets because they result from molar absorptivity curves that are indistinct, suggesting that there was no change in electronic structure upon binding.

False positives and false negatives are detrimental to scientific understanding. The association of molecules with each other is, in a sense, the essence of chemistry. To be misled about binding undermines the integrity of human understanding regarding chemical systems. It is becoming increasingly unacceptable to publish binding studies that have not been properly vetted. Therefore, it is vital to employ statistical tools to delineate experiments that evidence binding justifiably from ones that only appear to do so.

Acknowledgements

Funding: This work is supported by the National Science Foundation through an RUI grant from the Division of Chemistry (2004005). We are also grateful to the STEAM Ahead program of the state of Michigan for supporting A.E.B. and A.A.S.

Supporting Information

The Supporting Information includes an Excel spreadsheet containing all datasets as well as a text file containing summary information on all datasets and their respective fittings.

References

1) Neves, S.R.; Ram, P.T.; Iyengar, R. G Protein Pathways. *Science* **2002**. [online] 296 (5573), 1636–1639. doi.org/10.1126/science.1071550.

2) Patt, J. et al. An experimental strategy to probe Gq contribution to signal transduction in living cells*, J. Biol. Chem.* **2021,** 296, 100472, doi.org/10.1016/j.jbc.2021.100472.

3) Kostenis, E.; Pfeil, E.M.; Annala, S. Heterotrimeric Gq proteins as therapeutic targets? *J. Biol. Chem.* **2020,** 295, 5206-5215, doi.org/10.1074/jbc.REV119.007061.

4) Klepac, K. et al. The Gq signalling pathway inhibits brown and beige adipose tissue. *Nat. Commun*. **2016,** 7, 10895, doi.org/10.1038/ncomms10895.

5) Grace P.M. et al. DREADDed microglia in pain: implications for spinal inflammatory signaling in male rats. *Exp. Neurol.* **2018,** 304, 125-131, doi.org/10.1016/j.expneurol.2018.03.005.

6) Sanchez, J.; Holmgren, J. Cholera toxin - a foe & a friend, *Indian J. Med. Res*. **2011**, *133,* 153-163.

7) Mangmool, S.; Kurose, H. G(i/o) protein-dependent and -independent actions of Pertussis Toxin (PTX), *Toxins (Basel),* **2011**, *3,* 884-899.

8) Nishimura, A.; Kitano, K.; Takasaki, J.; Taniguchi, M.; Mizuno, N.; Tago, K.; Hakoshima, T.; Itoh, H. Structural basis for the specific inhibition of heterotrimeric G q protein by a small molecule. *Proc. Nat. Acad. Sci.* **2010**, 107(31), 13666–13671. doi.org/10.1073/pnas.1003553107.

9) Schrage, R. et al. The experimental power of FR900359 to study Gq-regulated biological processes. *Nat. Commun*. **2015**, *6*, 10156, doi.org/10.1038/ncomms10156.

10) Raniolo, S.; Limongelli, V. Ligand binding free-energy calculations with Funnel Metadynamics. *Nat. Protoc.* **2020**. 15: 2837-2866. *ISSN 1750-2799*, doi.org/10.1038/s41596-020-0342-4.

11) Limongelli, V.; Bonomi, M.; Parrinello, M. Funnel metadynamics as accurate binding free-energy method. *Proc. Natl. Acad. Sci. U. S. A*. **2013**, 110, 6358-6363. *ISSN: 0027-8424,* doi.org/10.1073/pnas.1303186110

12) Thordarson, P. Binding Constants and Their Measurement. *Supramol. Chem*. **2012**.

13) Vander Griend, D. A.; Bediako, D. K.; DeVries, M. J.; DeJong, N. A.; Heeringa, L. P. Detailed Spectroscopic, Thermodynamic, and Kinetic Characterization of Nickel(II) Complexes with 2, 2'-Bipyridine and 1, 10-Phenanthroline Attained via Equilibrium-Restricted Factor Analysis. *Inorg. Chem*. **2008**, *47* (2), 656–662. doi.org/doi: 10.1021/ic700553d.

14) Thordarson, P. Determining Association Constants from Titration Experiments in Supramolecular Chemistry. *Chem. Soc. Rev.* **2011**, *40* (3), 1305–1323. doi.org/10.1039/C0CS00062K.

15) Baranauskienė, L.; Petrikaitė, V.; Matulienė, J.; Matulis, D. Titration Calorimetry Standards and the Precision of Isothermal Titration Calorimetry Data. *Int J Mol Sci* **2009**, *10* (6), 2752–2762. doi.org/10.3390/ijms10062752.

16) Tellinghuisen, J. Stupid Statistics! *Methods Cell Biol*. **2008**, *84*, 739–780. doi.org/10.1016/S0091-679X(07)84023-4.

17) Bastos, M.; Abian, O.; Johnson, C. M.; Ferreira-da-Silva, F.; Vega, S.; Jimenez-Alesanco, A.; Ortega-Alarcon, D.; Velazquez-Campoy, A. Isothermal Titration Calorimetry. *Nat Rev Methods Primers* **2023**, *3* (1), 1–23. doi.org/10.1038/s43586-023-00199-x.

18) Li, Q.; Kang, C. A Practical Perspective on the Roles of Solution NMR Spectroscopy in Drug Discovery. *Molecules* **2020**, *25* (13), 2974. doi.org/10.3390/molecules25132974.

19) Caricato, M.; Coluccini, C.; Vander Griend, D. A.; Forni, A.; Pasini, D. From Red to Blue Shift: Switching the Binding Affinity from the Acceptor to the Donor End by Increasing the π-Bridge in Push–Pull Chromophores with Coordinative Ends. *New J. Chem*. **2013**, *37* (9), 2792–2799. doi.org/10.1039/C3NJ00466J.

20) Etkind, S. I.; Vander Griend, D. A.; Swager, T. M. Electroactive Anion Receptor with High Affinity for Arsenate. *J. Org. Chem*. **2020**, *85* (15), 10050–10061. doi.org/10.1021/acs.joc.0c01206.

21) Li, Y.; Vander Griend, D. A.; Flood, A. H. Modelling Triazolophane-Halide Binding Equilibria Using Sivvu Analysis of UV-Vis Titration Data Recorded under Medium Binding Conditions. *Supramol. Chem*. **2009**, *21* (1–2), 111–117. doi.org/10.1080/10610270802527051.

22) Mocz, G.; Ross, J. A. Fluorescence Techniques in Analysis of Protein-Ligand Interactions. *Methods Mol. Biol*. **2013**, *1008*, 169–210. doi.org/10.1007/978-1-62703-398-5_7.

23) Rossi, A. M.; Taylor, C. W. Analysis of Protein-Ligand Interactions by Fluorescence Polarization. *Nat. Protoc.* **2011**, *6* (3), 365–387. doi.org/10.1038/nprot.2011.305.

24) Möller, M.; Denicola, A. Study of Protein-Ligand Binding by Fluorescence. *Biochem. Mol. Biol. Ed.* **2002**, *30* (5), 309–312. doi.org/10.1002/bmb.2002.494030050089.

25) Rodger, A.; Marrington, R.; Roper, D.; Windsor, S. Circular Dichroism Spectroscopy for the Study of Protein-Ligand Interactions. In *Protein-Ligand Interactions: Methods and Applications*; Ulrich Nienhaus, G., Ed.; Humana Press: Totowa, NJ, **2005**, 343–363. doi.org/10.1385/1-59259-912-5:343.

26) Wetzel, W. Using Thermostable Raman Interaction Profiling (TRIP) For Protein Binding Screening. **2024**, *39*, 16–17.

27) Bowlby, B. Studying protein–ligand binding with Raman spectroscopy. *BioTechniques*. www.biotechniques.com/analytical-chemistry/sartorius_sptl_molecular_interactions_studying-protein-ligand-binding-with-raman-spectroscopy/ (accessed 2024-07-19).

28) Lorenz-Fonfria, V. A. Infrared Difference Spectroscopy of Proteins: From Bands to Bonds. *Chem. Rev.* **2020**, *120* (7), 3466–3576. doi.org/10.1021/acs.chemrev.9b00449.

29) Hirose, K. *Anal. Methods in Supramol. Chem.* Schalley, C. A., Ed.; Wiley-VCH: Weinheim, 2007.

30) Kazmierczak, N. P.; Chew, J. A.; Michmerhuizen, A. R.; Kim, S. E.; Drees, Z. D.; Rylaarsdam, A.; Thong, T.; Laar, L. V.; Griend, D. A. V. Sensitivity Limits for Determining 1:1 Binding Constants from Spectrophotometric Titrations via Global Analysis. *J. Chemom.* **2019**, *33* (5), e3119. doi.org/10.1002/cem.3119.

31) Kazmierczak, N. P.; Vander Griend, D. A. Properly Handling Negative Values in the Calculation of Binding Constants by Physicochemical Modeling of Spectroscopic Titration Data. *J. Chemom.* **2019**, *33* (11), 3183–3196. doi.org/10.1002/cem.3183.

32) Hibbert, D. B.; Thordarson, P. The Death of the Job Plot, Transparency, Open Science and Online Tools, Uncertainty Estimation Methods and Other Developments in Supramolecular Chemistry Data Analysis. *Chem. Commun.* **2016**, *52* (87), 12792–12805. doi.org/10.1039/C6CC03888C.

33) Evstigneev, M. P.; Buchelnikov, A. S.; Kostjukov, V. V.; Pashkova, I. S.; Evstigneev, V. P. Indistinguishability of the Models of Molecular Self-Assembly. *Supramol. Chem.* **2013**, *25* (4), 199–203. doi.org/10.1080/10610278.2012.752090.

34) Jarmoskaite, I.; AlSadhan, I.; Vaidyanathan, P. P.; Herschlag, D. How to Measure and Evaluate Binding Affinities. *eLife* **2020**, *9*, e57264. doi.org/10.7554/eLife.57264.

35) Jameson, L. P.; Smith, N. W.; Dzyuba, S. V. Dye-Binding Assays for Evaluation of the Effects of Small Molecule Inhibitors on Amyloid (Aβ) Self-Assembly. *ACS Chem. Neurosci.* **2012**, *3* (11), 807–819. doi.org/10.1021/cn300076x.

36) Zhou, G.; Lu, X.; Yuan, M.; Li, T.; Li, L. Enzymatic Cycle-Inspired Dynamic Biosensors Affording No False-Positive Identification. *Anal. Chem.* **2021**, *93* (46), 15482–15492. doi.org/10.1021/acs.analchem.1c03502.

37) Deng, N.; Forli, S.; He, P.; Perryman, A.; Wickstrom, L.; Vijayan, R. S. K.; Tiefenbrunn, T.; Stout, D.; Gallicchio, E.; Olson, A. J.; Levy, R. M. Distinguishing Binders from False Positives by Free Energy Calculations: Fragment Screening Against the Flap Site of HIV Protease. *J. Phys. Chem. B* **2015**, *119* (3), 976–988. doi.org/10.1021/jp506376z.

38) Wallace, R. M. ANALYSIS OF ABSORPTION SPECTRA OF MULTICOMPONENT SYSTEMS1. *The Journal of Physical Chemistry* **1960**, *64* (7), 899–901. https://doi.org/doi: 10.1021/j100836a019.

39) Wallace, R. M. ANALYSIS OF ABSORPTION SPECTRA OF MULTICOMPONENT SYSTEMS1. *J. Phys. Chem.* **1960**, *64* (7), 899–901. doi.org/doi: 10.1021/j100836a019.

40) Gampp, H.; Maeder, M.; Meyer, C. J.; Zuberbühler, A. D. Calculation of Equilibrium Constants from Multiwavelength Spectroscopic Data--I: Mathematical Considerations. *Talanta* **1985**, *32* (2), 95–101. doi.org/10.1016/0039-9140(85)80035-7.

41) Sajjadi, S. M.; Abdollahi, H. Hard–Soft Modeling Parallel Factor Analysis to Solve Equilibrium Processes. *J. Chemom.* **2011**, *25* (4), 169–182. doi.org/10.1002/cem.1341.

42) Vander Griend, D.A.; DeVries, M. J.; Greeley, M. Sivvu, **2006**.

43) Kazmierczak, N. P.; Chew, J. A.; Vander Griend, D. A. Bootstrap Methods for Quantifying the Uncertainty of Binding Constants in the Hard Modeling of Spectrophotometric Titration Data. *Anal. Chim. Acta* **2022**, *1227*, 339834. doi.org/10.1016/j.aca.2022.339834.

44) Ludden, T. M.; Beal, S. L.; Sheiner, L. B. Comparison of the Akaike Information Criterion, the Schwarz Criterion and the F Test as Guides to Model Selection. *J. Pharmacokinet. and Biopharm.* **1994**, *22* (5), 431–445. doi.org/10.1007/BF02353864.

45) DeSa, R. J.; Matheson, I. B. C. A Practical Approach to Interpretation of Singular Value Decomposition Results. *Meth. Enzymol.* **2004**, *384*, 1–8. doi.org/10.1016/S0076-6879(04)84001-1.

46) Bardsley, W. G.; McGinlay, P. B. The Use of Non-Linear Regression Analysis and the F Test for Model Discrimination with Dose-Response Curves and Ligand Binding Data. *J. Theor. Biol.* **1987**, *126* (2), 183–201. doi.org/10.1016/S0022-5193(87)80228-X.

47) Rouder, J. N.; Engelhardt, C. R.; McCabe, S.; Morey, R. D. Model Comparison in ANOVA. *Psychon. Bull. Rev.* **2016**, *23* (6), 1779–1786. doi.org/10.3758/s13423-016-1026-5.

48) Glatting, G.; Kletting, P.; Reske, S. N.; Hohl, K.; Ring, C. Choosing the Optimal Fit Function: Comparison of the Akaike Information Criterion and the F-Test. *Med. Phys.* **2007**, *34* (11), 4285–4292. doi.org/10.1118/1.2794176.

49) Nielsen, J. K.; Christensen, M. G.; Jensen, S. H. Bayesian Model Comparison and the BIC for Regression Models. In *2013 IEEE Int. Conf. Acoust. Speech Signal Process* **2013**, 6362–6366. doi.org/10.1109/ICASSP.2013.6638890.

50) *Model Selection and Multimodel Inference*; Burnham, K. P., Anderson, D. R., Eds.; Springer New York: New York, NY, 2004. https://doi.org/10.1007/b97636.

51) Burnham, K. P.; Anderson, D. R. Multimodel Inference: Understanding AIC and BIC in Model Selection. *Sociological Methods & Research* **2004**, *33* (2), 261–304. https://doi.org/10.1177/0049124104268644.

52) Aho, K.; Derryberry, D.; Peterson, T. Model Selection for Ecologists: The Worldviews of AIC and BIC. *Ecology* **2014**, *95* (3), 631–636.

53) Burguillo, F. J.; Wright, A. J.; Bardsley, W. G. Use of the F Test for Determining the Degree of Enzyme-Kinetic and Ligand-Binding Data. A Monte Carlo Simulation Study. *Biochem. J.* **1983**, *211* (1), 23–34. doi.org/10.1042/bj2110023.

54) Peterson, Y. K.; Bernard, M. L.; Ma, H.; Hazard, S.; Graber, S. G.; Lanier, S. M. Stabilization of the GDP-Bound Conformation of Giα by a Peptide Derived from the G-Protein Regulatory Motif of AGS3 *. *J. Biol. Chem.* **2000**, *275* (43), 33193–33196. doi.org/10.1074/jbc.C000509200.

55) Private communication with the Limongelli lab

56) Higashijima, T.; Ferguson, K. M.; Sternweis, P. C.; Smigel, M. D.; Gilman, A. G. Effects of Mg2+ and the Beta Gamma-Subunit Complex on the Interactions of Guanine Nucleotides with G Proteins. *J. Biol. Chem.* **1987**, *262* (2), 762–766. doi.org/10.1016/S0021-9258(19)75851-7.